ФИЗИКА ЭЛЕМЕНТАРНЫХ ЧАСТИЦ И АТОМНОГО ЯДРА
2014. Т. 45. ВЫП. 3

MEMORY EFFECTS IN NUCLEAR FERMI LIQUID

V. M. Kolomietz

Institute for Nuclear Research, Kiev

ФИЗИКА ЭЛЕМЕНТАРНЫХ ЧАСТИЦ И АТОМНОГО ЯДРА
2014. Т. 45. ВЫП. 3

MEMORY EFFECTS IN NUCLEAR FERMI LIQUID

V. M. Kolomietz

Institute for Nuclear Research, Kiev

The kinetic theory is applied to the nuclear Fermi liquid. The nuclear collective dynamics is treated in terms of the observable variables: particle density, current density, pressure, etc. The influence of Fermi-surface distortion, relaxation processes and memory effects on the nuclear dynamics is studied. We show that the presence of the dynamic Fermi-surface distortion gives rise to some important consequences in the nuclear dynamics which are absent in classical liquids. We discuss the nuclear small amplitude excitations, the spinodal instability, the nuclear fission and the bubble instability in heated Fermi liquid in the presence of the memory effects.

Кинетическая теория применена для описания ядерной ферми-жидкости. Динамика ядра описывается в терминах наблюдаемых величин: плотности частиц, плотности тока, давления и т. п. Исследуется влияние на динамику ядра эффектов искажения поверхности Ферми, процессов релаксации и эффектов памяти. Показано, что присутствие динамического искажения поверхности Ферми приводит к ряду важных следствий в ядерной динамике, которые отсутствуют в классической жидкости. Мы обсуждаем возбуждение ядра при малых амплитудах, спинодальную неустойчивость, деление ядер и пузырьковую неустойчивость в нагретой ферми-жидкости в присутствии эффектов памяти.

PACS: 24.10.Cn; 21.60.Ev; 24.10.Nz; 24.30.Cz; 24.75+i

INTRODUCTION

The theoretical study of many-particle systems implies two essential ingredients: the knowledge of the interparticle interaction and the technics to solve the many-body Shrödinger equation. In the case of the presence of a small parameter (e.g., fine-structure constant in atomic physics or quantum electrodynamics), the quntum-mechanical perturbation theory can be effectively applied whereas the variational approaches are more proper in the case of strong interparticle interaction. A significant feature of a nucleus is that the free-space nucleon–nucleon interaction is strongly renormalized inside the nucleus. This fact leads to the additional difficulties in a solving of the nuclear many-body problem because its description requires the use of some effective nucleon–nucleon interaction which cannot be established from the first principle. Moreover, the effective nucleon–nucleon interaction depends usually on the nucleon surroundings and becomes an object of the variational procedure also [1].

Note that due to the use of the effective interaction, the equation of state (EOS) for nuclei shows the saturated behavior which is similar to the classical

van der Waals equation of state. In particular, the nuclear matter evolves through the phase-separation and spinodal instability boundaries and may exhibit the first- and second-order (liquid-gas) phase transitions [2]. Note also that the study of nuclear many-body systems within the variational approaches subsided by the effective nucleon–nucleon interaction has a conceptual advantage because allows one to connect the fundamental nuclear characteristics such as the EOS with basic first principles.

One of the most intriguing problems of modern nuclear physics is the investigation of nuclear collective dynamics [3]. In general, the collective motion of the nuclear Fermi liquid is influenced strongly by the Fermi motion of nucleons and is accompanied by the dynamic distortion of the Fermi surface in the momentum space [4]. The presence of the dynamic Fermi-surface distortion gives rise to some important consequences in the nuclear dynamics which are absent in classical liquids. The dynamics of a nuclear Fermi liquid is determined by the pressure tensor instead of the scalar pressure as in a classical liquid. This fact changes the conditions for the propagation of the isoscalar and isovector sound excitations and creates a strong transverse component in the velocity field of the particle flow. Furthermore, because of the Fermi-surface distortion, the scattering of particles on the distorted Fermi surface becomes possible and the relaxation of collective motion occurs [5]. The equations of motion of nuclear Fermi liquid take then a non-Markovian form. The memory effects depend here on the relaxation time and provide a connection between both limiting cases of the classical liquid (short relaxation time limit) and the quantum Fermi liquid (long relaxation time limit). The Markovian dynamics only exists in these two limiting cases.

The below-used approach is the macroscopic one and involves into consideration the equations of motion for the macroscopic observable values such as the particle density or the nuclear shape parameters. Note that both the macroscopic and microscopic approaches can be effectively used to study the nuclear collective motion. The main theoretical approaches to the microscopic description of nuclear collective excitations are based upon the Random Phase Approximation (RPA), which is, essentially, the linear approximation to the time-dependent Hartree–Fock theory [3]. We note also the microscopic quasiparticle–phonon approach which was successfully used by the V. G. Soloviev's group in Dubna [6] to describe the nuclear low-lying state as well as the Giant Multipole Resonance (GMR) region.

In this article, we will pay close attention to the nuclear dynamics starting from the self-consistent mean-field approximation and the collisional kinetic theory. The interparticle interaction enters into consideration in both the self-consistent mean field and the collision integral. The nuclear dynamics is determined then in terms of local collective variables such as the mean particle density, velocity field, pressure tensor, etc. The key elements of this approach are the Fermi motion of nucleons and the Fermi-surface distortion which lead to

the memory effects on the nuclear dynamics. We note that taking into consideration the Fermi-surface distortion effects allows the description of a new class of phenomena, most famous of which are Giant Multipole Resonances (GMR). Furthermore, a scattering of particles on the distorted Fermi surface gives rise to the fluid viscosity. We will show that the development of instability in nuclear processes like binary fission or multifragmentation in heavy-ion reactions also depends significantly on the dynamic Fermi-surface distortion.

1. COLLISIONAL KINETIC EQUATION AND FLUID DYNAMICS APPROACH

In the present paper, we will follow the Boltzmann–Vlasov kinetic theory for the Wigner distribution function taking into consideration the Fermi-surface distortions and the relaxation processes caused by the interparticle collision on the distorted Fermi surface [5]. There are at least two advantages of the kinetic approach to the quantum many-body problem: (i) In contrast to the quantum Shrödinger equation, the kinetic equation incorporates the damping effects because of the relaxation processes. Note that for the quantum approach it cannot be achieved directly because of Hermitian's condition for the quantum Hamiltonian. (ii) The kinetic equation can be easily generalized to the case of finite temperature T, whereas the temperature cannot be implanted straight to the quantum equations of motion. The semiclassical kinetic approach to the nuclear dynamics was widely used in many studies. One can mention here the direct solution of the semiclassical Boltzmann–Vlasov kinetic equation [7] and the use of the method based on the phase-space moments of the Wigner distribution function [8, 9].

We are starting from the self-consistent Boltzmann–Vlasov kinetic equation in the following form [5]:

$$\frac{\partial}{\partial t} f + \frac{\mathbf{p}}{m} \cdot \boldsymbol{\nabla}_r f - \boldsymbol{\nabla}_r V \cdot \boldsymbol{\nabla}_p f = \mathrm{St}\,[f], \tag{1}$$

where $f \equiv f(\mathbf{r}, \mathbf{p}; t)$ is the Wigner distribution function; $V \equiv V(\mathbf{r}, \mathbf{p}; t)$ is the self-consistent mean field and $\mathrm{St}\,[f]$ is the collision integral. The momentum distribution is distorted during the time evolution of the system and the distribution function takes the form

$$f(\mathbf{r}, \mathbf{p}; t) = f_{\mathrm{sph}}(\mathbf{r}, \mathbf{p}; t) + \sum_{l \geqslant 1} \delta f_l(\mathbf{r}, \mathbf{p}; t), \tag{2}$$

where $f_{\mathrm{sph}}(\mathbf{r}, \mathbf{p}; t)$ describes the spherical distribution in momentum space and l is the multipolarity of the Fermi-surface distortion. We point out that the widely-used time-dependent Thomas–Fermi (TDTF) approximation and the corresponding nuclear liquid-drop model (LDM) are obtained from Eq. (1) if one takes the

distribution function $f(\mathbf{r},\mathbf{p};t)$ in the following restricted form: $f_{\rm TF}(\mathbf{r},\mathbf{p};t) = f_{\rm sph}(\mathbf{r},\mathbf{p};t) + \delta f_{l=1}(\mathbf{r},\mathbf{p};t)$ instead of Eq. (2), see [10]. Below we will extend the TDTF approximation taking into account the dynamic Fermi-surface distortion up to multipolarity $l = 2$ [11, 12]. We will also assume that the collective motion is accompanied by a small deviation of the momentum distribution from the spherical symmetry, i.e., even in the case of large amplitude motion, the main contribution to the distribution function $f(\mathbf{r},\mathbf{p};t)$ is given by the Thomas–Fermi term $f_{\rm TF}(\mathbf{r},\mathbf{p};t)$ and the additional term $\delta f_{l=2}(\mathbf{r},\mathbf{p};t)$ provides the small corrections only. The lowest orders $l = 0$ and 1 of the Fermi-surface distortion (which are not necessary small) do not contribute to the collision integral because of the conservation laws [5], and the linearized collision integral with respect to small perturbation $\delta f_{l=2}(\mathbf{r},\mathbf{p};t)$ is given by

$$\mathrm{St}\,[f] = -\frac{\delta f_{l=2}}{\tau}, \tag{3}$$

where τ is the relaxation time.

An additional advantage of the kinetic approach is the possibility of reducing the kinetic equation (1) to the macroscopic equations of motion for the observable values. One of such a kind examples gives the transition from Eq. (1) to the equations of motion for the local values like particle density

$$\rho \equiv \rho(\mathbf{r},t) = \int \frac{g\ d\mathbf{p}}{(2\pi\hbar)^3} f(\mathbf{r},\mathbf{p};t),$$

velocity field

$$\mathbf{u} \equiv \mathbf{u}(\mathbf{r},t) = \frac{1}{\rho}\int \frac{g d\mathbf{p}}{(2\pi\hbar)^3}\,\frac{\mathbf{p}}{m} f(\mathbf{r},\mathbf{p};t),$$

and pressure tensor

$$P_{\nu\mu} \equiv P_{\nu\mu}(\mathbf{r},t) = \frac{1}{m}\int \frac{g d\mathbf{p}}{(2\pi\hbar)^3}(p_\nu - mu_\nu)(p_\mu - mu_\mu) f(\mathbf{r},\mathbf{p};t),$$

where g is the spin–isospin degeneracy factor. Taking the first three moments in $\mathbf{p}$ space from the kinetic equation (1), one can obtain [4]:

(i) Continuity equation

$$\frac{\partial}{\partial t}\rho + \nabla_\nu(\rho u_\nu) = 0. \tag{4}$$

(ii) Euler-like equation

$$m\rho\frac{\partial}{\partial t}u_\nu + m\rho\nabla_\mu u_\nu u_\mu + \nabla_\nu P + \rho\nabla_\nu\frac{\delta E_{\rm pot}}{\delta\rho} = -\nabla_\mu P_{\nu\mu}, \tag{5}$$

where $E_{\rm pot}$ is the potential energy of the interparticle interaction.

(iii) Memory equation

$$\frac{\partial}{\partial t}P'_{\nu\mu} + P\frac{\partial}{\partial t}\Lambda_{\nu\mu} = -\frac{1}{\tau}P'_{\nu\mu}, \tag{6}$$

where $P \equiv P(\mathbf{r},t)$ is the isotropic part of the pressure tensor

$$P(\mathbf{r},t) = \frac{1}{3m}\int \frac{gd\mathbf{p}}{(2\pi\hbar)^3}p^2 f_{\rm sph}(\mathbf{r},\mathbf{p};t),$$

$P'_{\nu\mu} \equiv P'_{\nu\mu}(\mathbf{r},t)$ is the deviation of the pressure tensor from its isotropic part, $P(\mathbf{r},t)$, due to the Fermi-surface distortion

$$P'_{\nu\mu}(\mathbf{r},t) = \frac{1}{m}\int \frac{d\mathbf{p}}{(2\pi\hbar)^3}(p_\nu - mu_\nu)(p_\mu - mu_\mu)\delta f_{l=2}(\mathbf{r},\mathbf{p};t),$$

and $\epsilon_{\rm pot}$ is the potential energy density related to the self-consistent mean field V as $V = \delta\epsilon_{\rm pot}/\delta\rho$. The tensor $\Lambda_{\nu\mu}$ in Eq. (6) is given by

$$\Lambda_{\nu\mu} = \nabla_\nu\chi_\mu + \nabla_\mu\chi_\nu - \frac{2}{3}\delta_{\nu\mu}\nabla_\lambda\chi_\lambda,$$

where $\chi_\nu \equiv \chi_\nu(\mathbf{r},t)$ is the displacement field related to the velocity field as $u_\nu \equiv u_\nu(\mathbf{r},t) = \partial\chi_\nu(\mathbf{r},t)/\partial t$.

From Eq. (6) we find the pressure tensor which is given by the following form:

$$P'_{\nu\mu}(\mathbf{r},t) = P'_{\nu\mu}(\mathbf{r},t_0) - \int\limits_{t_0}^{t} dt' \, \exp\left(\frac{t'-t}{\tau}\right) P(\mathbf{r},t')\frac{\partial}{\partial t'}\Lambda_{\nu\mu}(\mathbf{r},t'). \tag{7}$$

The tensor $P'_{\nu\mu}(\mathbf{r},t_0)$ is determined by the initial conditions. In the case of the quadrupole distortion of the Fermi surface, the tensor $P'_{\nu\mu}(\mathbf{r},t_0)$ is derived by the initial displacement field $\chi_\nu(\mathbf{r},t_0)$.

Collecting Eqs. (5) and (7), we obtain the basic equation of the fluid dynamics approach (FDA) in the following form (we assume here the initial condition $P'_{\nu\mu}(\mathbf{r},t_0) = 0$ for simplicity):

$$m\rho\frac{\partial}{\partial t}u_\nu + m\rho\nabla_\mu u_\nu u_\mu + \nabla_\nu P + \rho\nabla_\nu\frac{\delta E_{\rm pot}}{\delta\rho} - \\ - \nabla_\mu \int\limits_{t_0}^{t} dt' \, \exp\left(\frac{t'-t}{\tau}\right) \, P(\mathbf{r},t')\frac{\partial}{\partial t'}\Lambda_{\nu\mu}(\mathbf{r},t') = 0. \tag{8}$$

Here and in the further similar expressions, the repeated Greek indices are to be understood as summed over. Equation (8) represents the non-Markovian, Navier–Stokes-like equation of motion. The integral (the so-called memory integral) in the

right-hand side of Eq. (8) occurs due to the Fermi-distortion effect, i.e., due to the term $\delta f_{l=2}(\mathbf{r}, \mathbf{p}; t)$. This effect affects the nuclear dynamics extremely strongly. It can be easily seen that in the limit of short relaxation time $\tau \to 0$, Eq. (8) is reduced to the classical viscous Navier–Stokes equation. In the general case, the memory integral in Eq. (8) gives rise to both the time irreversible viscosity and to the additional, time-dependent conservative force, see below.

2. SMALL AMPLITUDE DYNAMICS

Considering a small amplitude motion, we will linearize Eq. (8) with respect to the small variations of particle density $\delta\rho(\mathbf{r}, t)$ and the displacement field $\chi_\nu(\mathbf{r}, t)$. Assuming also the periodic motion with $\delta\rho(\mathbf{r}, t) \sim \exp(-i\omega t)$ and using the continuity equation (4), we obtain from Eq. (8) the following equation of motion for the Fourier transform $\chi_{\nu,\omega} \equiv \chi_{\nu,\omega}(\mathbf{r})$ of the displacement field:

$$-\rho_{\rm eq}\omega^2\chi_{\nu,\omega} + \hat{L}\chi_{\nu,\omega} = \nabla_\mu \sigma_{\nu\mu,\omega}, \tag{9}$$

where the conservative terms are abbreviated by

$$\hat{L}\chi_{\nu,\omega} = -\frac{1}{m}\rho_{\rm eq}\nabla_\nu \left[\frac{\delta^2 E_{\rm pot}}{\delta\rho^2}\right]_{\rm eq} \nabla_\mu \rho_{\rm eq}\chi_{\mu,\omega} - {\rm Im}\left(\frac{\omega\tau}{1-{\rm i}\omega\tau}\right)\nabla_\mu \frac{{\rm P_{eq}}}{\rm m}\Lambda_{\nu\mu,\omega}.$$

Here and below the subscript «eq» means the equilibrium. In particular,

$$\rho_{\rm eq} \equiv \rho_{\rm eq}(\mathbf{r}) = \int \frac{g\, d\mathbf{p}}{(2\pi\hbar)^3} f_{\rm eq}(\mathbf{r}, \mathbf{p}),$$
$$P_{\rm eq} \equiv P_{\rm eq}(\mathbf{r}) = \frac{1}{3m}\int \frac{g\, d\mathbf{p}}{(2\pi\hbar)^3} p^2 f_{\rm eq}(\mathbf{r}, \mathbf{p}; t).$$

In Eq. (9), $\sigma_{\nu\mu}$ is the viscosity tensor

$$\sigma_{\nu\mu,\omega} = -i(\omega/m)\eta_\omega \Lambda_{\nu\mu,\omega},$$

where the viscosity coefficient

$$\eta_\omega = {\rm Re}\left(\frac{\tau}{1-i\omega\tau}\right) P_{\rm eq}.$$

We will demonstrate applications of Eq. (9) which are related to the nuclear collective motion.

2.1. Compression Zero- and First-Sound Modes. The equation of motion (9) is closed. It can be applied to both the isoscalar and isovector sound excitations. We will consider the Fermi surface distortion and the memory effects on the isoscalar compression mode. To simplify the problem, we will assume

the constant equilibrium bulk density $\rho_{\rm eq}(\mathbf{r}) = \rho_0 = {\rm const}$. Using the continuity equation (4), we obtain from Eq. (9) the equation for the density variation $\delta\rho = -\nabla_\nu(\rho_{\rm eq}\chi_\nu)$ in the following form [13]:

$$\omega^2\delta\rho + \left(\frac{K'_\omega}{9m}\right)\nabla^2\delta\rho = i\omega\left(\frac{4\eta_\omega}{3m\rho_{\rm eq}}\right)\nabla^2\delta\rho. \tag{10}$$

Here

$$K'_\omega = K + 8\left(\frac{\epsilon_{\rm kin}}{\rho}\right)_{\rm eq}{\rm Im}\left(\frac{\omega\tau}{1-i\omega\tau}\right), \tag{11}$$

where $\epsilon_{\rm kin}$ is the kinetic energy density and K is the incompressibility of nuclear matter

$$K \equiv 9\rho_0^2\left(\frac{\delta^2 E_{\rm pot}/A}{\delta\rho^2}\right)_{\rm eq}.$$

The result of Eq. (11) can be interpreted as a renormalization of the Fermi-liquid incompressibility caused by both the Fermi-surface distortions and the memory effects in Eq. (8). Thus, there is a significant difference between the static nuclear incompressibility coefficient, K, i.e., derived as a stiffness coefficient with respect to a change in the bulk density, and the dynamic one, of Eq. (11), associated with the sound propagation. This difference is due to the second term on the RHS of Eq. (11) caused by the Fermi-surface distortion effects. The quantity η_ω in Eq. (10) determines the time-irreversible contribution to the pressure tensor $P'_{\alpha\beta}$ and can be considered as the viscosity coefficient due to the relaxation occurring on the distorted Fermi surface. Expression (10) is valid independently of the nucleon's collision rate. The viscosity goes to zero in both the rare, $\tau \to \infty$, and frequent, $\tau \to 0$, collision limits.

Assuming a plane wave solution $\delta\rho \sim \exp(i\mathbf{q}\cdot\mathbf{r} - \mathbf{i}\omega\mathbf{t})$ one obtains from Eq. (10) the following dispersion relation:

$$\omega^2 = \left(\frac{K'_\omega}{9m}\right)q^2 - i\omega\left(\frac{4\eta_\omega}{3m\rho_{\rm eq}}\right)q^2. \tag{12}$$

The solution of this equation defines the complex wave number q (ω is real). A simple solution to Eq. (12) can be obtained in two limiting cases of the frequent collision (first sound) regime, $\omega\tau \to 0$, and the rare collision (zero sound) regime, $\omega\tau \to \infty$. The sound velocity $u = \omega/q$ is given by

$$u = u_1 = \sqrt{\frac{K}{9m}} \ \text{ if } \ \omega\tau \to 0 \ \text{ and by } \ u = u_0 = \sqrt{\frac{K+\Delta K}{9m}} \ \text{ if } \ \omega\tau \to \infty, \tag{13}$$

where $\Delta K \approx 8(\epsilon_{\rm kin}/\rho)_{\rm eq} \approx (24/5)\epsilon_F \approx 200$ MeV (we adopted the kinetic Fermi energy $\epsilon_F \approx 40$ MeV). We point out that the value of ΔK is comparable

with the static incompressibility $K \approx 220$ MeV and we have $u_0 \approx \sqrt{2}u_1$. The factor $\sqrt{2}$ in this relation is due to the restriction $\ell \leqslant 2$ for the multipolarity ℓ of the Fermi-surface distortion. In a general case of arbitrary ℓ this factor is increased to $\sqrt{3}$ [14]. The result (13) means that in contrast to the first sound (frequent collision) regime, the sound velocity of the compression mode cannot, in general, be used directly to extract the static incompressibility of K because of the additional contribution from the Fermi-surface distortion effects which result in the renormalization of the incompressibility K into K'_ω. Note also that the viscosity η_ω of the Fermi liquid disappears in both limiting cases of the frequent and rare collisions, see above the derivation of η_ω,

$$\eta_\omega \sim \tau \quad \text{if} \quad \omega\tau \to 0 \quad \text{and} \quad \eta_\omega \sim 1/\tau \quad \text{if} \quad \omega\tau \to \infty.$$

Using both asymptotic sound velocity u_1 and u_0, the solution to the dispersion relation (12) can be written as

$$q = \frac{\omega}{u_0}(n + i\kappa),$$

where the refraction coefficient n and the attenuation coefficient κ (both real) are obtained from the following equation:

$$n + i\kappa = \sqrt{\frac{1 - i\omega\tau}{(u_1/u_0)^2 - i\omega\tau}}. \tag{14}$$

In the frequent collision (first sound) regime we obtain from Eq. (14)

$$n = \frac{u_0}{u_1}, \quad \kappa = \omega\tau \left(\frac{u_0}{2u_1}\right) \left[\left(\frac{u_0}{u_1}\right)^2 - 1\right] \quad \text{if} \quad \omega\tau \ll 1.$$

In the opposite case of the rare collision (zero sound) regime we obtain

$$n = 1, \quad \kappa = \left[1 - \left(\frac{u_1}{u_0}\right)^2\right] / (2\omega\tau) \quad \text{if} \quad \omega\tau \gg 1.$$

The attenuation coefficient κ in both limiting regimes is a complicated function of the frequency because of the retardation effect (ω dependency) in the relaxation time τ [14]. In the case of sound propagation in a hot nuclear matter, the competition between the temperature smoothing effects in the equilibrium distribution function f_{eq} and the dynamic distortions of the particle momentum distribution leads to the following expression for the relaxation time [14]:

$$\tau = \frac{\hbar\tau_0}{(\hbar\omega)^2 + (2\pi T)^2}, \tag{15}$$

where T is the temperature of nuclear matter and τ_0 is the constant which depends on the in-medium nucleon–nucleon cross section.

In Fig. 1, we have plotted both coefficients n and κ as obtained from Eqs. (14) and (15). In the high-temperature limit, the system goes to the frequent collision (first sound) regime with the saturated refraction coefficient $n \approx u_0/u_1 \approx \sqrt{3}$ (we use the factor $\sqrt{3}$ instead of $\sqrt{2}$ assuming the contribution of the higher multipolarities $\ell > 2$ in the Fermi-surface distortion as was mentioned above) and the attenuation coefficient $\kappa \sim \tau \sim 1/T^2$. In the opposite low temperature limit, the system is close to the zero sound regime with $n \approx 1$. We point out a shift of both n and κ by nonzero values at $T \to 0$. This is due to the memory effect in the relaxation time τ of Eq. (15): in the very high frequency limit, the system can exist close to the first sound regime at $n \approx \sqrt{3}$ even at zero temperature. The position of the maximum of $\kappa(T)$ in Fig. 1 can be interpreted as the transition temperature $T_{\rm tr}$ of zero- to first-sound regimes in a hot Fermi system. The value of $T_{\rm tr}$ depends slightly on the sound frequency ω and it is shifted to smaller values with the increase of ω.

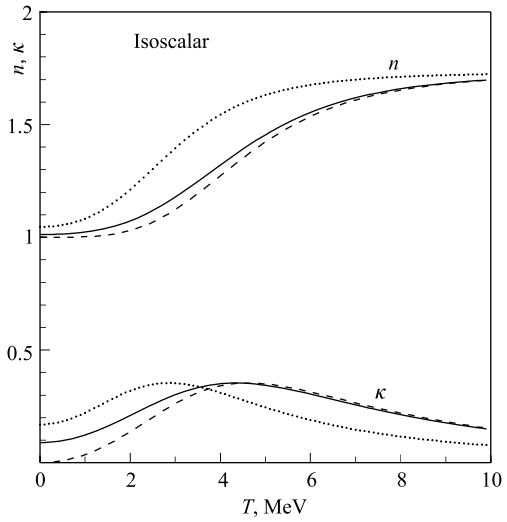

Fig. 1. The refraction, n, and the attenuation, κ, coefficients of the isoscalar sound wave as functions of temperature T. The calculation was performed for two eigenenergies $\hbar\omega = 1$ MeV (solid line) and $\hbar\omega = 1$ eV (dashed line). The dotted line was obtained with the vacuum nucleon–nucleon cross section for $\hbar\omega = 1$ MeV

In conclusion to this section, we would like to note again that there is a significant difference between the static nuclear incompressibility coefficient, K, i.e., derived as a stiffness coefficient with respect to a change in the bulk density, and the dynamic one, K'_ω, associated with the zero sound velocity, see Eq. (11). This difference occurs due to the memory and the Fermi-surface distortion effect on the Fermi-liquid dynamics. The Fermi-surface distortion

phenomenon is responsible for the collisional relaxation of the collective modes in a Fermi liquid and for the non-Markovian character of the nuclear matter viscosity (memory effect in the viscosity η_ω, Eq. (8)). The memory effects in the viscosity play an essential role in the description of the temperature dependence of the refraction coefficient n. We note also the bell-shaped form of the attenuation coefficient κ as a function of the temperature T, see Fig. 1. This peculiarity of $\kappa(T)$ provides a new criterion for the determination of the transition temperature $T_{\rm tr}$ between the zero-sound and first-sound regimes in hot nuclear matter.

2.2. Incompressible Fermi Liquid. Isoscalar Giant Quadrupole Resonance. For the description of shape oscillations of a certain multipolarity L of a liquid drop of radius $R(t)$ we specify the liquid surface as

$$\rho = \rho_0 \Theta(R(t) - r),$$

where

$$R(t) = R_{\rm eq}\left[1 + \sum_M \alpha_{\rm LM}(t)\, Y_{\rm LM}(\theta, \phi)\right].$$

We will assume that the liquid is incompressible, $\nabla_\nu \chi_\nu = 0$, and irrotational, $\boldsymbol{\nabla} \times \chi = 0$. The displacement field $\chi_\nu(\mathbf{r}, t)$ can be written then in the following form:

$$\chi_\nu(\mathbf{r}, t) = \sum_M a_{{\rm LM},\nu}(\mathbf{r})\, \alpha_{\rm LM}(t),$$

where

$$a_{{\rm LM},\nu}(\mathbf{r}) = \frac{1}{L R_0^{L-2}} \nabla_\nu (r^L Y_{\rm LM}(\theta, \phi)).$$

Multiplying Eq. (9) by $m a^*_{{\rm LM},\nu}$, summing over ν and integrating over $\mathbf{r}$ space, we obtain the equation of motion for the Fourier transform of the collective variables $\alpha_{\rm LM}(t)$ [12],

$$-\omega^2 B_L \alpha_{{\rm LM},\omega} + (C_L^{\rm (LDM)} + C'_L)\alpha_{{\rm LM},\omega} - i\omega\gamma_L(\omega)\alpha_{{\rm LM},\omega} = 0. \qquad (16)$$

The collective mass B_L is found to be

$$B_L = m \int d\mathbf{r}\, \rho_{\rm eq} \sum_\nu |a_{{\rm LM},\nu}|^2 = \frac{3}{4\pi L} A m R_{\rm eq}^2.$$

The static (ω-independent) stiffness coefficient $C_L^{\rm (LDM)}$ of the liquid drop model is given by [15, 16]

$$C_L^{\rm (LDM)} = \frac{1}{4\pi}(L-1)(L+2) b_S A^{2/3} - \frac{5}{2\pi}\frac{L-1}{2L+1} b_C \frac{Z^2}{A^{1/3}},$$

where b_S and b_C are the surface energy and the Coulomb energy coefficients appearing in the nuclear mass formula, respectively. We point out that the nucleon–nucleon interaction, manifested at the starting equations (8), is presented in Eq. (16) only implicitly through the phenomenological stiffness coefficient $C_L^{(\mathrm{LDM})}$.

At finite frequencies ω, the distortion of the Fermi surface causes an additional contribution, C'_L in Eq. (16), to the stiffness coefficient. It is found as

$$C'_L \equiv C'_L(\omega) = \mathrm{Im}\left(\frac{\omega\tau}{1-i\omega\tau}\right)\int d\mathbf{r}\, P_{\mathrm{eq}}\overline{\Lambda}^{(\mathrm{LM})}_{\nu\mu}\nabla_\mu a^*_{\mathrm{LM},\nu}, \tag{17}$$

where

$$\overline{\Lambda}^{(\mathrm{LM})}_{\nu\mu} = \nabla_\nu a_{\mathrm{LM},\mu} + \nabla_\mu a_{\mathrm{LM},\nu}.$$

Using derivation of $a_{\mathrm{LM},\nu}$, we obtain for the integral in Eq. (17)

$$\int d\mathbf{r}\, \rho_{\mathrm{eq}}\overline{\Lambda}^{(\mathrm{LM})}_{\nu\mu}\nabla_\mu a^*_{\mathrm{LM},\nu} = 2\rho_0\frac{(L-1)(2L+1)}{L}R_0^3$$

and

$$C'_L(\omega) = d_L\,\mathrm{Im}\left(\frac{\omega\tau}{1-i\omega\tau}\right)P_{\mathrm{eq}}.$$

The proportionality to $(\omega\tau)^2$, for small values of this product, explains, why such a correction does not appear in the hydrodynamic limit $\omega\tau \to 0$.

For the friction coefficient $\gamma_L(\omega)$ in Eq. (16) we obtain

$$\gamma_L(\omega) = \eta_\omega\int d\mathbf{r}\,\overline{\Lambda}^{(\mathrm{LM})}_{\nu\mu}\nabla_\mu a^*_{\mathrm{LM},\nu} = 2\frac{(L-1)(2L+1)}{L}R_0^3\,\eta_\omega.$$

The friction coefficient $\gamma_L(\omega)$ disappears in two limiting cases of the frequent collision (first sound) regime, $\omega\tau \to 0$, and the rare collision (zero sound) regime, $\omega\tau \to \infty$. Both, C'_L and γ_L depend implicitly on the temperature via the T dependence of the relaxation time τ in Eq. (15).

The homogeneous equation of motion (16) provides the following secular equation for the surface eigenvibrations:

$$-\omega^2 B_L + \left(C_L^{(\mathrm{LDM})} + C'_L(\omega)\right) - i\,\omega\,\gamma_L(\omega) = 0. \tag{18}$$

The transport coefficients $C'_L(\omega)$ and $\gamma_L(\omega)$ are ω-dependent because of the memory effects. To solve Eq. (18), both the coefficients have to be defined in the complex ω plane through analytical continuation of the corresponding expressions for $C'_L(\omega)$ and $\gamma_L(\omega)$.

Assuming the zero-sound regime $\omega\tau \to \infty$ and $\gamma_L(\omega) = 0$, the eigenfrequencies of shape vibrations are derived by the following transcendental equation:

$$-\omega^2 B_L + \left(C_L^{(\mathrm{LDM})} + C'_L(\omega)\right) = 0, \tag{19}$$

with $\mathrm{Im}\,\omega = 0$. The energy of the surface eigenmode of the incompressible Fermi-liquid drop is given by

$$\hbar\omega_L = \hbar\sqrt{\frac{C_L^{(\mathrm{LDM})} + C'_L(\omega_L)}{B_L}}. \tag{20}$$

Usually one has $C_L^{(\mathrm{LDM})} \ll C'_L$ and Eq. (20) leads to the following A dependence of the energy of the surface eigenmode:

$$\hbar\omega_L \sim A^{-1/3}.$$

This is in contrast to the prediction of the traditional liquid drop model [16], where

$$\hbar\omega_L^{(\mathrm{LDM})} = \hbar\sqrt{\frac{C_L^{(\mathrm{LDM})}}{B_L}} \sim A^{-1/2}.$$

The inclusion of the Fermi-surface distortion term $C'_L(\omega)$ into the eigenenergy (20) is crucially important for correct description of the centroid energies of the nuclear isoscalar giant multipole resonances with $L \geqslant 2$, within a fluid

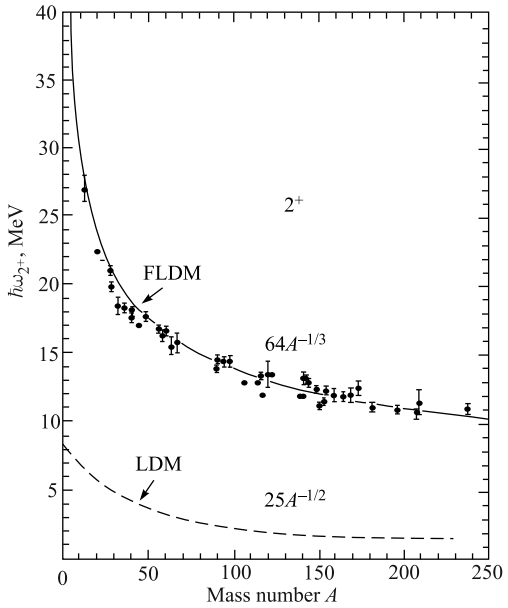

Fig. 2. Dependence of the energy $\hbar\omega_{2^+}$ of nuclear strong collectivized isoscalar 2^+ excitations (isoscalar giant quadrupole resonance) on the mass number A. The dashed line is for the liquid drop model and the solid line is for the Fermi-liquid drop where the Fermi-surface distortion effects are taken into account

dynamic approach. As an example, we consider the quadrupole mode $L = 2$. In Fig. 2, we show the result of calculation of the energy of quadrupole eigenvibrations (isoscalar giant quadrupole resonance) within the Fermi-liquid drop model (FLDM) given by Eq. (20) (solid line) and the traditional liquid-drop model energy $\hbar\omega_L^{(\mathrm{LDM})}$ (dashed line) [15, 16]. Here we have adopted the Fermi energy $\epsilon_F = 40$ MeV. The FLDM result agrees very well with the experimental value of the energy of the isoscalar quadrupole resonance $\hbar\omega_{2^+}^{\mathrm{exp}} \approx 63A^{-1/3}$ MeV. One can see also that the traditional liquid-drop model contradicts significantly the experimental data for $\hbar\omega_{2^+}^{\mathrm{exp}}$. Discussing the Giant Multipole Resonance phenomenon, it is necessary to recall the pioneer work [17] by A. B. Migdal on the phenological description of the Isovector Giant Dipole Resonance (IGDR). Migdal's work represents one of the first usages of the liquid-drop model to study the nuclear collective dynamics. This idea was intensively used later in many applications to the nuclear fission and the tests of different approaches to the problem of Giant Multipole Resonances. Actually, in the present paper, we extend Migdal's conception taking into consideration the nucleon Fermi motion in nuclear Fermi-liquid drop.

3. SPINODAL INSTABILITY

With decreasing bulk density or increasing internal excitation energy (temperature) the liquid drop (saturated many-body system) reaches the regions of mechanical or thermodynamical instabilities with respect to small density fluctuations (spinodal instability). We will here consider the peculiarities of development of the spinodal instability in a Fermi-liquid drop mainly focussing on the boundary conditions and the memory effects. We will take into account the relaxation and the dynamic Fermi-surface distortions and compare both regimes of the frequent and rare collisions.

Let us consider small density fluctuations. Using the continuity equation (4), we will rewrite Eq. (9) in the following form:

$$m\,\frac{\partial^2}{\partial t^2}\,\delta\rho = \nabla_\nu \rho_{\mathrm{eq}} \nabla_\nu \frac{\delta E}{\delta \rho} + \nabla_\nu \nabla_\mu P'_{\nu\mu}. \tag{21}$$

The pressure tensor $P'_{\nu\mu}$ can be expressed through the displacement field $\chi_\nu(\mathbf{r}, t)$, see Eq. (7). Assuming also $\delta\rho \sim \mathrm{e}^{-i\omega t}$, the Fourier transform $P'_{\nu\mu,\omega}$ to the pressure tensor $P'_{\nu\mu}$ is given by

$$P'_{\nu\mu,\omega} = \frac{i\omega\tau}{1 - i\omega\tau} P_{\mathrm{eq}} \Lambda_{\nu\mu,\omega}.$$

Below, we will use the extended Thomas–Fermi approximation for the internal kinetic energy [3] and the Skyrme-type forces for the interparticle interaction [18].

The equation of state then reads

$$E[\rho] = \int d\mathbf{r} \left\{ \frac{\hbar^2}{2\,m} \left[\frac{3}{5} \left(\frac{3\pi^2}{2} \right)^{2/3} \rho^{5/3} + \frac{1}{4}\,\eta_W \frac{(\boldsymbol{\nabla}\rho)^2}{\rho} \right] + \right.$$
$$\left. + \frac{3}{8}\,t_0\,\rho^2 + \frac{1}{16}\,t_3\,\rho^3 + \frac{1}{64}\,(9\,t_1 - 5\,t_2)(\boldsymbol{\nabla}\rho)^2 \right\},$$

where t_k are the Skyrme-force parameters and η_W is the Weizsäcker correction to kinetic energy density for the finite Fermi system. Note that the Skyrme-force parameters t_k are connected with the Landau scattering amplitudes [14] by the following relation:

$$F_0 = \frac{9\,\rho_0}{8\,\epsilon_F} \left[t_0 + \frac{3}{2}\,t_3\,\rho_0 \right] \frac{m^*}{m} + 3 \left(1 - \frac{m^*}{m} \right), \quad F_1 = 3 \left(\frac{m^*}{m} - 1 \right),$$

where m^* is the effective nucleon mass and

$$\frac{m}{m^*} = 1 + \frac{m\,\rho_0}{8\,\hbar^2}\,(3\,t_1 + 5\,t_2).$$

We will assume a sharp surface behavior of $\rho_{\rm eq}$ having a bulk density ρ_0 and an equilibrium radius R_0. Taking into account the continuity equation (4), the equation of motion (21) is reduced in the nuclear interior to the following form (we consider the isoscalar mode) [19]:

$$-m\,\omega^2\,\delta\rho = \left(\frac{1}{9}\,K - \frac{4}{3}\frac{i\omega\tau}{1 - i\omega\tau} \left(\frac{P_{\rm eq}}{\rho_0} \right) \right) \nabla^2\delta\rho - 2(\beta + t_s\,\rho_0)\,\nabla^2\nabla^2\delta\rho, \quad (22)$$

where

$$\beta = \frac{\hbar^2}{8\,m}\,\eta_W, \quad t_s = \frac{1}{64}\,(9\,t_1 - 5\,t_2).$$

We note the presence of the anomalous dispersion term in Eq. (22) (last term on the r.h.s). This term contains both the Weizsäcker correction to the kinetic energy density (the term with β) and the potential energy contribution due to the momentum dependence in the effective Skyrme forces (the term with t_s). Both of them contribute to the nuclear surface energy. At the saturated nuclear density, $\rho_0 = \rho_{\rm sat} \approx 0.17$ fm^{-3}, the potential energy term $\sim t_s\,\rho_0$ gives the dominant contribution. However, for decreasing density ρ_0 the potential term goes down and becomes comparable with the Weizsäcker correction term for the bulk density $\rho_{0,\rm crit} \approx 0.3\,\rho_{\rm sat}$ used below in numerical calculations. We point out that the anomalous dispersion term in Eq. (22) removes the unphysical infinite growth rate of short-wavelength fluctuations of the particle density, occurring in

the case of infinite nuclear matter with $t_1 = t_2 = 0$. The solution to Eq. (22) for a fixed multipolarity L is given by

$$\delta\rho(\mathbf{r}, t) = \rho_0\, j_L(qr)\, Y_{\mathrm{LM}}(\theta, \phi)\, \alpha_{\mathrm{LM}}(t),$$

where q is the wave number and $\alpha_{\mathrm{LM}}(t)$ is the amplitude of the density oscillations. We will distinguish between stable and unstable regimes of density fluctuations. In the case of a stable mode at $K > 0$, a solution of Eq. (22) leads to the following dispersion relation:

$$\omega^2 = u^2 q^2 - i\omega \frac{\gamma(\omega)}{m} q^2 + \kappa_s q^4. \tag{23}$$

Here, u is the sound velocity

$$u^2 = u_1^2 + \kappa_v,$$

u_1 is the velocity of the first sound

$$u_1^2 = \frac{1}{9m}\, K,$$

$\gamma(\omega)$ is the friction coefficient

$$\gamma(\omega) = \frac{4}{3}\mathrm{Re}\left[\frac{\tau}{1 - \mathrm{i}\omega\tau}\right] \frac{\mathrm{P_{eq}}}{\rho_0},$$

and

$$\kappa_v = \frac{4}{3}\mathrm{Im}\left[\frac{\omega\tau}{1 - \mathrm{i}\omega\tau}\right] \frac{\mathrm{P_{eq}}}{\mathrm{m}\rho_0}, \quad \kappa_{\mathrm{s}} = \frac{2}{\mathrm{m}}\,(\beta + \mathrm{t_s}\rho_0).$$

The quantities κ_v and $\gamma(\omega)$ appear due to the Fermi-surface distortion effect. The dispersion relation (23) determines both the real and the imaginary part of the eigenfrequency ω.

Let us consider now the volume instability regime, $K < 0$, and introduce a growth rate $\Gamma = -i\omega$ (Γ is real, $\Gamma > 0$). Using Eq. (23), one obtains

$$\Gamma^2 = |u_1|^2\, q^2 - \zeta(\Gamma)\, q^2 - \kappa_s\, q^4, \tag{24}$$

where

$$\zeta(\Gamma) = \frac{4}{3m}\frac{\Gamma\tau}{1 + \Gamma\tau}\frac{P_{\mathrm{eq}}}{\rho_0}.$$

The dispersion equation (24) is valid for arbitrary relaxation time τ and includes the influence of the collisional relaxation and the memory effects on the bulk instability. It allows us to consider both the frequent and the rare interparticle collision regimes for the instability growth rate.

(i) Frequent collision regime: $\Gamma\tau \to 0$.

The contribution from the dynamic distortion of the Fermi surface, κ_v, can be neglected in this case and we have from Eq. (24)

$$\Gamma^2 = |u_1|^2\, q^2 - \Gamma \left(\frac{\tilde{\gamma}}{m}\right) q^2 - \kappa_s\, q^4, \tag{25}$$

where $\tilde{\gamma} = (8/15)\epsilon_F \tau$ is the friction coefficient. In the case of small friction coefficient $\tilde{\gamma}$, one obtains from Eq. (25)

$$\Gamma^2 \approx |u_1|^2 q^2 - \kappa_s q^4 - \frac{\tilde{\gamma}}{m}\, q^2 \sqrt{|u_1|^2 q^2 - \kappa_s q^4}. \tag{26}$$

The amplitude of the density oscillations, $\delta\rho_L(\mathbf{r}, t)$, grows exponentially if $\Gamma > 0$. Expression (26) determines two characteristic values of the wave number q, namely, $q_{\max}$, where the growth rate reaches a maximum of $\Gamma_{\max}$, and $q_{\rm crit}$, where Γ goes to zero, i.e.,

$$\Gamma = \Gamma_{\max} \quad \text{at} \quad q = q_{\max} < q_{\rm crit}, \quad \text{and} \quad \Gamma = 0 \quad \text{at} \quad q = q_{\rm crit}.$$

The values of $q_{\max}$ and $q_{\rm crit}$ are obtained from, see Eq. (26),

$$\left.\frac{\partial \Gamma}{\partial q}\right|_{q=q_{\max}} = 0 \quad \text{and} \quad q_{\rm crit}^2 = \frac{|u_1|^2}{\kappa_s} \quad \text{at} \quad u_1^2 < 0.$$

Thus, the critical wave number $q_{\rm crit}$ does not depend on the friction. However, the presence of friction reduces the instability, see also Fig. 3 below.

(ii) Rare collision regime: $\Gamma\tau \to \infty$.

In this case, we have from Eq. (24)

$$\Gamma^2 = |u_1|^2 q^2 - \kappa_v' q^2 - \kappa_s q^4,$$

where

$$\kappa_v' = \frac{4}{3m}\frac{P_{\rm eq}}{\rho_{\rm eq}}.$$

The critical value $q_{\rm crit}$ and the value $q_{\max}$ are given by

$$q_{\rm crit}^2 = \frac{|u_1|^2 - \kappa_v'}{\kappa_s}, \quad q_{\max}^2 = \frac{1}{2}\, q_{\rm crit}^2.$$

Thus, the distortion of the Fermi surface (presence of term κ_v' in $q_{\rm crit}$) leads to a decrease of the critical value $q_{\rm crit}$, i.e., the Fermi-liquid drop becomes more stable with respect to the bulk density fluctuations due to the dynamic Fermi-surface distortion effects.

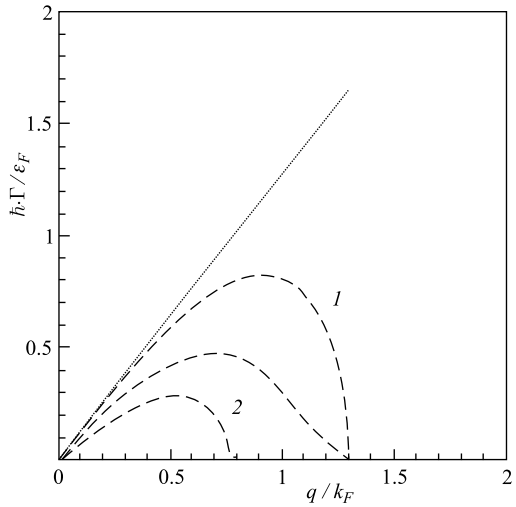

Fig. 3. The dependence of the instability growth rate Γ on the wave number q in units of Fermi wave number $k_F = p_F/\hbar$. The calculations were performed for the Skyrme force, temperature $T = 6$ MeV, bulk density $\rho_0 = 0.3\rho_{\rm eq}$ with $\rho_{\rm eq} = 0.145$ fm^{-3} and relaxation time parameter $\tau_0 = 9.2$ MeV^{-1}. The solid curve is for the Fermi-liquid drop (Eq. (24)) which takes into account the anomalous dispersion term $\sim q^4$ and the memory effects. The dashed curves are the results for the nonviscous liquid: curve *1* is for the usual liquid, i.e., neglecting the Fermi-surface distortion effects, and curve *2* is for the Fermi liquid. The straight line is for infinite nuclear matter, i.e., neglecting anomalous dispersion term $\sim q^4$ in Eq. (24)

In Fig. 3, we show the instability growth rate Γ as obtained from Eq. (24). We also show in this figure the result for the nonviscous infinite nuclear matter neglecting the anomalous dispersion term $\sim q^4$ and the nonviscous finite liquid drop neglecting the Fermi-surface distortion effects. In a finite system, the non-monotony behavior of the instability growth rate as a function of the wave number q is due to the anomalous dispersion term $\sim q^4$ in Eq. (24) created by the gradient terms in the equation of state. We point out that the finite system becomes more stable with respect to short-wave-length density fluctuations at $q > q_{\rm max}$. We can also see that the presence of viscosity (friction) decreases the instability and leads to a shift of the position of the maximum of $\Gamma(q)$ to the left. This means that the point from the left slope of curve $\Gamma(q)$ can appear on its right slope. This fact is essential for the derivation of the character of spinodal instabilities (fission or multifragmentation) in finite nuclei. Namely, the nucleus which is unstable with respect to the fission mode can become unstable to the multifragmentation due to the relaxation processes.

The position of the maximum of the instability growth rate $\Gamma(q)$ is shifted to a longer wavelength due to the Fermi surface distortion (FSD) effects (compare dashed curves *1* and *2* in Fig. 3). Thus, the most unstable mode is shifted to the region of the creation of larger clusters. Similarly to the above-mentioned viscosity effect on the instability growth rate $\Gamma(q)$, the FSD effects can change the position of q on the slopes of the curve $\Gamma(q)$, with respect to the position $q_{\max}$ of the maximum.

4. LARGE AMPLITUDE MOTION. NUCLEAR FISSION

The nuclear large amplitude dynamics, in particular nuclear fission, can be studied in terms of only a few collective variables like nuclear shape parameters [15]. Such a kind of approach is usually associated with the liquid drop model and its extensions and is acceptable for a slow collective motion, where the fast intrinsic degrees of freedom exert forces on the collective variables leading to a Markovian transport equation. An essential assumption is that the LDM provides a good approximation for a smooth part, $\widetilde{E}_{\rm pot}$, of the collective potential energy, $E_{\rm pot}$, and can be then used for the quantum calculations of $E_{\rm pot}$ within the shell-correction method [20], obtaining $E_{\rm pot} = \widetilde{E}_{\rm pot} + \delta\mathcal{U}$, where $\delta\mathcal{U}$ is the shell correction. On the other hand, it is well known (see also Fig. 2 above) that the LDM is not able to describe some strongly collective nuclear excitations such as the isoscalar giant multipole resonances. It is because the LDM ignores the important features of the nucleus as a Fermi liquid. In general, the collective motion of the nuclear Fermi liquid is accompanied by the dynamic distortion of the Fermi surface and the smooth energy $\widetilde{E}_{\rm pot}$ should be subsidized by an additional contribution, $\widetilde{E}_{{\rm pot},F}$, which is caused by the *dynamic* Fermi-surface distortion effect and is absent in the standard LDM [11, 12]. We point out that the energy $\widetilde{E}_{{\rm pot},F}$ is a smooth quantity (in the sense of the shell-correction method) and it cannot be recovered by taking into consideration the quantum shell corrections to the adiabatic (static) potential energy deformation.

Assuming that the nucleus is an incompressible and irrotational fluid with a sharp surface in $\mathbf{r}$ space, we will reduce the local equation of motion (5) to the equations for the variables $q = \{q_1, q_2, \ldots, q_N\}$, that specify the shape of the nucleus. The continuity equation (4) has to be complemented by the boundary condition on the moving nuclear surface S. Below we will assume that the axially symmetric shape of the nucleus is defined by rotation of the profile function $\rho = Y(z, \{q_i(t)\})$ around the z axis in the cylindrical coordinates ρ, z, φ. The velocity of the nuclear surface is then given by [21]

$$u_S = \sum_{i=1}^{N} \bar{u}_i \dot{q}_i,$$

where

$$\bar{u}_i = \frac{\partial Y/\partial q_i}{\Lambda}, \quad \Lambda = \sqrt{1 + \left(\frac{\partial Y}{\partial z}\right)^2}.$$

The potential of the velocity field takes the form

$$\phi = \sum_{i=1}^{N} \overline{\phi}_i \, \dot{q}_i,$$

where the potential field $\overline{\phi}_i \equiv \overline{\phi}_i(\mathbf{r}, q)$ is determined by the equations of the following Neumann problem:

$$\nabla^2 \overline{\phi}_i = 0, \quad (\mathbf{n} \nabla \overline{\phi}_i)_S = \frac{1}{\Lambda} \frac{\partial Y}{\partial q_i}, \tag{27}$$

where $\mathbf{n}$ is the unit vector which is normal to the nuclear surface. Using Eqs. (4) and (5) with multiplying Eq. (5) by $\nabla_\mu \overline{\phi}_i$ and integrating over $\mathbf{r}$, one obtains

$$\sum_{j=1}^{N} \left[B_{ij}(q)\ddot{q}_j + \sum_{k=1}^{N} \frac{\partial B_{ij}}{\partial q_k} \dot{q}_j \dot{q}_k + \int_{t_0}^{t} dt' \exp\left(\frac{t'-t}{\tau}\right) \kappa_{ij}(t,t') \dot{q}_j(t') \right] = \\ = -\frac{\partial E_{\mathrm{pot}}(q)}{\partial q_i}. \tag{28}$$

Here $B_{ij}(q)$ is the inertia tensor

$$B_{ij}(q) = m\rho_0 \oint ds \, \bar{u}_i \overline{\phi}_j.$$

The adiabatic collective potential energy, $E_{\mathrm{pot}}(q)$, does not contain the contribution from the Fermi-surface distortion effect and it is given by

$$E_{\mathrm{pot}}(q) = \int d\mathbf{r} \, (\epsilon_{\mathrm{kin}}(\mathbf{r}, \mathrm{II}) + \epsilon_{\mathrm{pot}}(\mathbf{r}, \mathrm{II})).$$

The memory kernel $\kappa_{i,j}(t,t')$ in Eq. (28) is given by

$$\kappa_{ij}(t,t') = 2 \int d\mathbf{r} \, P(\mathbf{r}, q(t')) \left[\nabla_\nu \nabla_\mu \overline{\phi}_i(\mathbf{r}, q(t))\right] \left[\nabla_\nu \nabla_\mu \overline{\phi}_j(\mathbf{r}, q(t'))\right].$$

The displacement field $\chi_\nu(\mathbf{r}, q)$ and the potential field $\overline{\phi}_i \equiv \overline{\phi}_i(\mathbf{r}, q)$ are determined by a solution to the Neumann problem (27). In the one-dimensional case and the irrotational flow, Eq. (27) leads to a velocity field potential of quadrupole type [21]

$$\phi(\mathbf{r}, q) = \frac{1}{4q}(2z^2 - x^2 - y^2).$$

In this case $q = q(t)$ is the dimensionless elongation of the figure in units of the radius $R_0 = r_0 A^{1/3}$ of the nucleus, and the basic equation of motion (28) takes the following form [22]:

$$B(q)\ddot{q} + \frac{\partial B(q)}{\partial q}\dot{q}^2 = -\frac{\partial E_{\rm pot}(q)}{\partial q} - \int_{t_0}^{t} dt' \exp\left(\frac{t'-t}{\tau}\right)\ \kappa(t,t')\ \dot{q}(t'). \qquad (29)$$

Here, the mass parameter $B(q)$ and the memory kernel $\kappa(t,t')$ are given by

$$B(q) = \frac{1}{5}\,AmR_0^2\ \left(1 + \frac{1}{2q^3}\right) \quad \text{and} \quad \kappa(t,t') = \frac{\kappa_0}{q(t)q(t')},$$

where $\kappa_0 = (4/5m)\pi\rho_0 p_F^2 R_0^3$.

To illustrate the memory effect on the large amplitude motion, we will apply Eq. (29) to the motion from the barrier point to the «scission» point. Following the Kramers model, we will approximate the potential energy $E_{\rm pot}(q)$ by an upright oscillator $(1/2)C_{\rm LDM}(q-q_0)^2$ with $q_0 = 1$ and an inverted oscillator $E_f - (1/2)\widetilde{C}_{\rm LDM}(q-q_f)^2$ which are joined smoothly as shown in Fig. 4. We will consider the motion from the barrier point B to the «scission» point C. The behavior of $q(t)$ depends dramatically on the memory effects and the relaxation time. In Fig. 5, we show the result for two values of the relaxation time $\tau = 3 \cdot 10^{-23}$ s and $\tau = 4 \cdot 10^{-22}$ s.

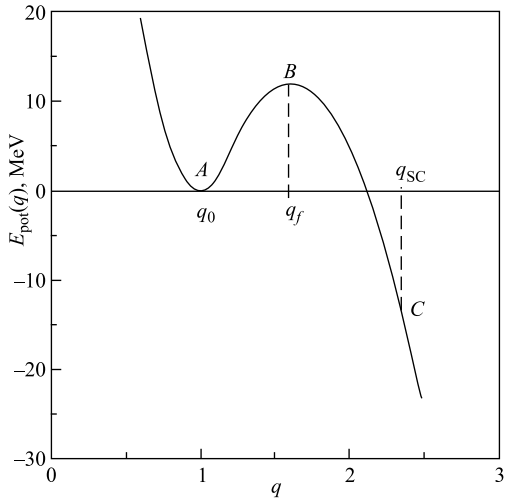

Fig. 4. Dependence of the potential energy $E_{\rm pot}(q)$ on the shape parameter q for the Kramers model. The dimensionless parameter q is the elongation of the figure in units of the radius $R_0 = r_0 A^{1/3}$ of the nucleus

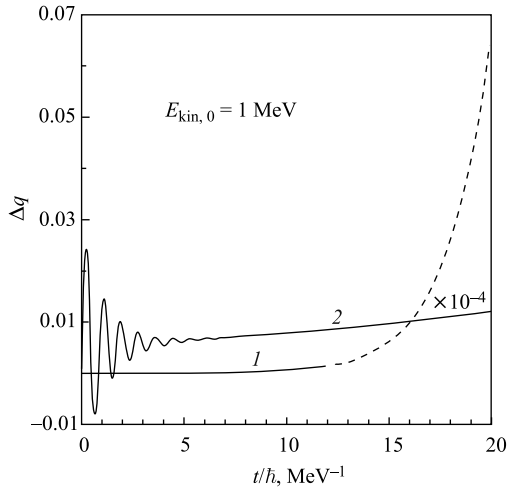

Fig. 5. Time variation of the change of the shape parameter Δq starting from the saddle point B (see Fig. 4), for various values of the relaxation time τ. The curves *1* and *2* correspond to the values of $\tau = 3 \cdot 10^{-23}$ s and $\tau = 4 \cdot 10^{-22}$ s, respectively. We have used the initial conditions $\Delta q(t_0) = 0$, $\Delta\dot{q}(t_0) = v_0$, and $\Delta\ddot{q}(t_0) = 0$ with the following parameters $q_f = 1.6$, $A = 236$, and $\hbar\omega_f = \hbar\sqrt{|\widetilde{C}_{\mathrm{LDM}}|/B_f} = 1.16$ MeV. The shape parameter q is dimensionless, see Fig. 4. The initial velocity v_0 was derived using the initial kinetic energy $E_{\mathrm{kin},0} = (1/2)B_f v_0^2 = 1$ MeV

In the case of the very short relaxation time, $\tau = 3 \cdot 10^{-23}$ s, the memory effects in Eq. (29) play a minor role only and the amplitude of motion is approximately an exponentially growing function, similar to the case of Newton motion from the barrier in the presence of the friction forces, see curve *1* in Fig. 5. The friction coefficient can be derived here from Eq. (29) at $\omega_{F,f}\tau \ll 1$ and it is given by $\gamma = \gamma_f = \kappa_f\tau = \omega_{F,f}^2 B_f \tau \sim \tau$, where $\omega_{F,f} = \sqrt{\kappa_f/B_f}$ is the characteristic frequency for the eigenvibrations caused by the Fermi-surface distortion effect. The behavior of $\Delta q(t)$ is changed significantly with an increase of the relaxation time. At large enough relaxation time, the descent from the barrier is accompanied by the damped oscillations (curve *2* in Fig. 5).

The origin of such a kind of oscillations is the following. It can be shown that the memory integral in Eq. (29) provides the conservative time-reversible (elastic) force $F_{i,\mathrm{cons}}$. The elastic force $F_{i,\mathrm{cons}}$ acts always *against* the driving force $-\partial E_{\mathrm{pot}}(q)/\partial q$. That creates the effect of the hindrance for the descent from the barrier B. This effect depends on both the collective velocity and the relaxation time. In the case of slow motion, the hindrance is absent similarly to the first sound regime for small amplitude vibrations. The hindrance effect grows if the collective velocity is growing. Due to this property, the velocity

of descent goes down, i.e., the hindrance effect becomes weaker and the nucleus starts to accelerate again, etc. Such a kind of change of the hindrance effect along the descent trajectory leads to the above-mentioned shape oscillations which accompany the descent of the nucleus from the fission barrier.

The memory integral in Eq. (29) contains also the time-irreversible part providing the damping (friction). The friction coefficient is essentially different in both above-mentioned regimes. In the rare collision regime $\omega_{F,f}\tau \gg 1$, the friction coefficient is obtained from Eq. (29) as $\gamma = \gamma_f = B_f/\tau \sim 1/\tau$. This behavior is opposite to the τ dependence of $\gamma_f \sim \tau$ in the frequent collision regime $\omega_{F,f}\ \tau \ll 1$. Such a feature of friction coefficient γ is a consequence of the memory effects in the Fermi liquid. To connect both limiting cases of rare and frequent collisions, there can be used the following bell-shaped extrapolation form for the friction coefficient:

$$\gamma = \gamma_f = \omega_{F,f} B_f \ \frac{\omega_{F,f}\tau}{1 + (\omega_{F,f}\tau)^2}. \tag{30}$$

Both the friction force $\sim \gamma_f$ and the elastic force $F_{i,\mathrm{cons}}(q,t)$ hinder the descent of the nucleus from the fission barrier. The elastic force $F_{i,\mathrm{cons}}(q,t)$ is due to the Fermi surface distortions and it is absent in the LDM. The presence of force $F_{i,\mathrm{cons}}(q,t)$ leads to an essential delay of the descent process with respect to the analogous result obtained from the Newton motion in the LDM. The influence of the memory effect on the descent time t_{sc} from the barrier to the

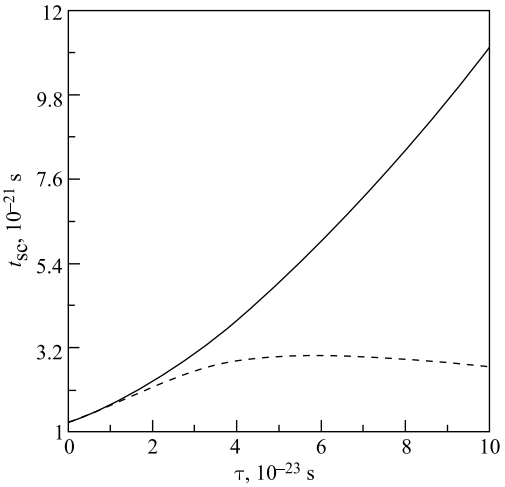

Fig. 6. Dependence upon relaxation time of the time, t_{SC}, required to travel a nucleus from the saddle point B to the «scission» point C (see Fig. 4). Solid line represents the result of the calculation in the presence of the memory effects and dashed line is for the case of Markovian (no memory) motion with the friction forces. The initial kinetic energy is $E_{\mathrm{kin}} = 1$ MeV

«scission» point $q_{\rm sc}$ is shown in Fig. 6. As is seen from Fig. 6, in the absence of the memory effects (dashed lines), the descent time $q_{\rm sc}$ is about $(1-3)\cdot 10^{-21}$ s and, as it should be, the value of $t_{\rm sc}$ goes to the limit of nonfriction motion for both the frequent collision regime, $\tau \to 0$, and the rare collision regime, $\tau \to \infty$. This property of the descent with no-memory effects is the result of the Fermi-liquid approximation (30) for the friction coefficient γ_f. In contrast to this Markovian motion, the non-Markovian descent time $t_{\rm sc}$ evaluated in the presence of the memory effects, i.e., in rare collision regime, grows monotonously with the relaxation time (see solid line in Fig. 6). The additional delay of the motion in the rare collision region is due to the contribution of the elastic force $F_{i,\rm cons}(q,t)$ and caused by the memory integral which acts against the driving force $-\partial E_{\rm pot}(q)/\partial q$.

5. BUBBLE INSTABILITY OF OVERHEATED NUCLEAR MATTER

Bellow we will consider the time development of the bubble instability in the thermodynamically metastable (overheated) nuclear matter. We will mainly focus on the dynamic effects related to the properties of the Fermi liquid. In particular, we will take into consideration the Fermi-surface distortion effects, memory effects (non-Markovian dynamics) and the relaxation processes in the boiled Fermi liquid.

The boiling process takes place in the form of the generation of vapor bubbles which then grow to macroscopic dimensions [23]. A liquid which is overheated in the usual sense, i.e., with respect to a phase separate by a plane surface, can be underheated with respect to a vapor bubble of a finite radius R. Let us consider the change of the free energy of the liquid due to the formation of a bubble of an arbitrary radius R (i.e., not necessary stable). At fixed pressure P, temperature T and isospin asymmetry parameter $X = (N-Z)/(N+Z)$, it is given by the change of the corresponding thermodynamical potential

$$\Delta\Phi = \Phi - \Phi_0.$$

Here $\Phi_0 = \overline{\mu}^{\rm liq}(A_{\rm liq} + A_{\rm vap})$ corresponds to the absence of the bubble, where $\overline{\mu}^{\rm liq}$ is the chemical potential of liquid phase, $A = N + Z$ is the number of nucleons. Here and below the indexes «liq» and «vap» denote the liquid and vapor phases, respectively. Taking into account that the surface free energy of the bubble is given by $4\pi R^2\sigma$, we will write, see [23],

$$\Delta\Phi = (\overline{\mu}^{\rm vap} - \overline{\mu}^{\rm liq})\frac{4\pi}{3}R^3\rho_{\rm vap} + 4\pi R^2\sigma,$$

where σ is the surface tension coefficient. At fixed P, T, and $X_{\rm liq}$, both chemical potentials $\overline{\mu}^{\rm vap}$ and $\overline{\mu}^{\rm liq}$ are also fixed and they are related to each other by the

equilibrium condition

$$\frac{\delta\Phi}{\delta A_{\rm liq}} = 0 \quad \text{at} \quad A_{\rm liq} + A_{\rm vap} = A = \text{const}, \tag{31}$$

where

$$\Phi = \overline{\mu}^{\rm liq} A_{\rm liq} + \overline{\mu}^{\rm vap} A_{\rm vap} + 4\pi R^2 \sigma. \tag{32}$$

Using Eqs. (31) and (32), one obtains (for metastable vapor phase $\overline{\mu}^{\rm vap} < \overline{\mu}^{\rm liq}$)

$$\overline{\mu}^{\rm liq} - \overline{\mu}^{\rm vap} = \frac{2\sigma}{\rho_{\rm vap} R^*}.$$

Here R^* is the radius of the so-called critical bubble which is given by [23, 24]

$$R^* = \frac{2\sigma T_0}{\rho_{\rm vap}\overline{\phi}(T - T_0)}, \tag{33}$$

where $\overline{\phi}$ is the latent heat of evaporation and T_0 is the temperature of saturated vapor in the case of plane geometry at a fixed pressure P_0. Finally, we obtain the following result for the change of the thermodynamical potential in the heated liquid:

$$\Delta\Phi \equiv \Delta\Phi(R) = 4\pi\sigma \left(R^2 - \frac{2R^3}{3R^*} \right). \tag{34}$$

In Fig. 7, we have plotted the thermodynamical potential as a function of the bubble radius (see Eq. (34)) for the overheated liquid nuclear matter with $T > T_0$

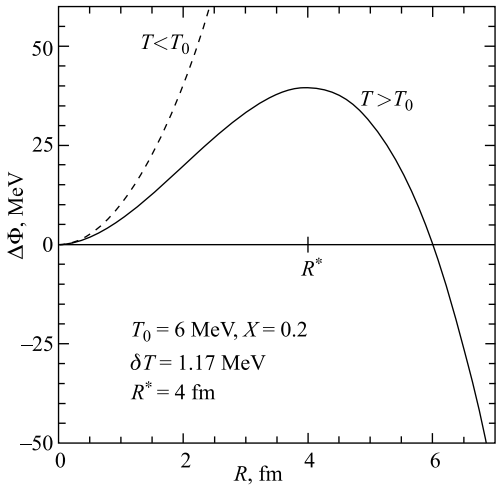

Fig. 7. Dependence of the thermodynamical potential (see Eq. (34)) of metastable Fermi liquid on the radius of the bubble. The solid line is for the overheated Fermi liquid with $T > T_0$ and the dashed line is for $T < T_0$

(solid curve) and for a temperature T below the boiling temperature T_0 (dashed curve). The position of the maximum of the curve $\Delta\Phi$ is located at $R = R^*$ and it is shifted to the left with the increase of the overheating temperature $\delta T = T - T_0$ because of Eq. (33). As one can see from Fig. 7, the point $R = R^*$ is the critical point for the metastable phase in the following sense: to start the boiling process, i.e., to start the process of increasing the size of the bubbles, the system must pass through the barrier $\Delta\Phi(R)$ to reach the region of $R > R^*$.

To describe the development of instability of the bubble with a nonequilibrium size $R > R^*$, one needs to know the equation of motion for the time-dependent bubble radius $R \equiv R(t)$. To obtain the macroscopic equation of motion for $R(t)$ in a heated Fermi liquid, we will start from the basic local equation of motion (8). A solution of the continuity equation (4) for the spherical bubble leads to the following displacement field in the surrounding liquid [25]:

$$\chi_\nu(r,t) = \frac{R^3}{3r^2}\frac{r_\nu}{r}, \quad r \geqslant R.$$

Multiplying Eq. (8) by $\bar{\chi}_\mu = u_\mu/\dot{R}$ and integrating over $\mathbf{r}$, one obtains the following non-Markovian equation for the collective variable $R(t)$, see also Eq. (29):

$$B\ddot{R} + \frac{1}{2}\frac{\partial B}{\partial R}\dot{R}^2 + \int_{t_0}^{t} dt' \dot{R}(t') \exp\left(\frac{t'-t}{\tau}\right) K(t,t') = -\frac{\partial E_{\rm pot}}{\partial R}. \qquad (35)$$

The inertial parameter B in Eq. (35) can be derived from the definition of the collective kinetic energy $E_{\rm kin}$. Namely,

$$E_{\rm kin} = \frac{m}{2}\int d\mathbf{r}\, \rho u^2 = \frac{1}{2} B \dot{R}^2.$$

Assuming $\rho_{\rm vap} \ll \rho_{\rm liq} \approx \rho = \rho_0 \theta(r - R)$, we obtain

$$B = 4\pi m \rho_0 R^3.$$

The collective potential energy $E_{\rm pot}(R)$ in Eq. (35) can be identified with the thermodynamical potential of Eq. (34):

$$E_{\rm pot}(R) = \Delta\Phi(R).$$

Finally, the memory kernel $K(t,t')$ in Eq. (35) is given by [26]

$$K(t,t') = \frac{32}{5}\pi\rho_0\epsilon_F R^2(t)/R(t').$$

We point out that the non-Markovian form of Eq. (35) is again due to the effects of the Fermi-surface distortion. Similarly to results of the previous section,

the memory integral in Eq. (35) provides both the friction and the conservative time-reversible force. For two limiting cases of rare ($\tau \to \infty$) and frequent ($\tau \to 0$) collision regimes, Eq. (35) is reduced to the standard Newton equation. For both limiting cases, we obtain from Eq. (35)

$$B^* \frac{\partial^2}{\partial t^2} R(t) = -k' R - \gamma \frac{\partial}{\partial t} R(t), \tag{36}$$

where $k' = k = \partial^2 \Delta\Phi(R)/\partial R^2 = -8\pi\sigma$ if $\tau \to 0$ and $k' = k + \widetilde{\kappa}$ if $\tau \to \infty$, where $\widetilde{\kappa} = (32/5)\pi\rho_0\epsilon_F R^*$. The friction coefficient γ in Eq. (36) can be derived similarly to γ_f in Eq. (30) and it is given by

$$\gamma = \omega_F B^* \frac{\omega_F \tau}{1 + (\omega_F \tau)^2},$$

which provides the correct limit for γ in both cases $\tau \to 0$ and $\tau \to \infty$. Here we have used the following notations: $\omega_F = \sqrt{\widetilde{\kappa}/B^*}$ and $B^* = 4\pi m \rho_0 R^{*3}$.

In Fig. 8, we show the solutions of both Eqs. (35) and (36) for $\Delta R(t) = R(t) - R^*$ in the case of descent from the right slope of the barrier $\Delta\Phi(R)$ for $R > R^*$. In the case of very short relaxation time $\tau \lesssim 3 \cdot 10^{-23}$ s (frequent collision regime), the memory effects in Eq. (35) play only a minor role (Markovian regime) and the amplitude of motion is approximately an exponentially growing function, similar to the case of Newton motion from the barrier in the presence

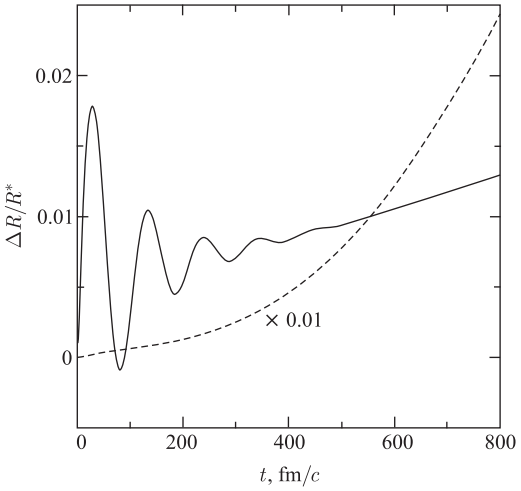

Fig. 8. Time variation of the bubble shape parameter R near the barrier point $R = R^*$ for various values of the relaxation time τ. The dashed and solid curves correspond to the values of $\tau = 3 \cdot 10^{-23}$ s obtained from Eq. (35) and $\tau = 4.5 \cdot 10^{-22}$ s obtained from Eq. (36), respectively

of the friction forces of Eq. (36), see dashed curve in Fig. 8. At large enough relaxation time, the bubble growth depends essentially on the memory effects (non-Markovian regime). The solid line in Fig. 8 shows $\Delta R(t)$ obtained from Eq. (35) for $\tau = 4.5 \cdot 10^{-22}$ s. As can be seen from Fig. 8, the behavior of $\Delta R(t)$ is changed dramatically with the increase of the relaxation time. For the large relaxation time, a significant time delay in the increase of the bubble size arises due to the non-Markovian effects. Moreover, the bubble growth is accompanied by damped oscillations. These oscillations are due to the memory integral in Eq. (35). The characteristic frequency, ω_R, and the corresponding damping parameter, ω_I, can be derived considering a small amplitude limit of Eq. (35) for the motion near the barrier point $R = R^*$. Assuming the small amplitude motion, we will look for the solution to Eq. (35) in the form

$$\Delta R = \sum_{i=1}^{3} C_i \exp(\lambda_i t),$$

where the coefficients C_i are determined by the initial conditions. Differentiating Eq. (35) over time we find that the eigenvalues λ_i can be obtained as solutions to the following secular equation:

$$\left(\lambda^2 + \frac{k}{B^*}\right)\left(\lambda + \frac{1}{\tau}\right) + \frac{\widetilde{\kappa}}{B^*}\lambda = 0. \tag{37}$$

In the case of the zero-relaxation-time limit, $\tau \to 0$, one obtains from Eq. (37) a nondamped motion with $\lambda = \pm\sqrt{|k|\ /B^*}$, i.e., the time evolution is derived by the static stiffness coefficients k. In an opposite case of rare collisions, $\tau \to \infty$, the solution to Eq. (37) leads to a motion with $\lambda = \pm i\sqrt{(-|k|\ + \widetilde{\kappa})/B^*}$. In contrast to the previous case, the additional contribution, $\widetilde{\kappa}$, appears at the stiffness coefficient $-|k|\ + \widetilde{\kappa}$ because of the Fermi surface distortion effect.

In a general case of arbitrary τ, the solution (35) for a small amplitude limit takes the form

$$\Delta R = C_\zeta\, \mathrm{e}^{\zeta t} + A_\omega\, \mathrm{e}^{-\Gamma t/2\hbar} \sin\left(\frac{Et}{\hbar}\right) + B_\omega\, \mathrm{e}^{-\Gamma t/2\hbar} \cos\left(\frac{Et}{\hbar}\right). \tag{38}$$

The characteristic frequency, ω_R, and the corresponding damping parameter, ω_I, can be derived from the imaginary and real parts of the complex conjugated roots of Eq. (37) as $\lambda = -\omega_I \pm i\omega_R$ with $\Gamma = 2\hbar\omega_I$ and $E = \hbar\omega_R$.

In Fig. 9, we show the dependence of the instability growth rate parameter ζ (see Eq. (38)), the energy of eigenvibrations E and the damping parameter Γ on the relaxation time τ. For small enough values of the relaxation time $\tau \lesssim 3 \cdot 10^{-23}$ s, the function $\Delta R(t)$ does not oscillate with time and it takes the following form (compare with Eq. (38) and see the dashed lines in Fig. 9):

$$\Delta R = C_\zeta\, \mathrm{e}^{\zeta t} + C_1\, \mathrm{e}^{-\Gamma_1 t/2\hbar} + C_2\, \mathrm{e}^{-\Gamma_2 t/2\hbar}. \tag{39}$$

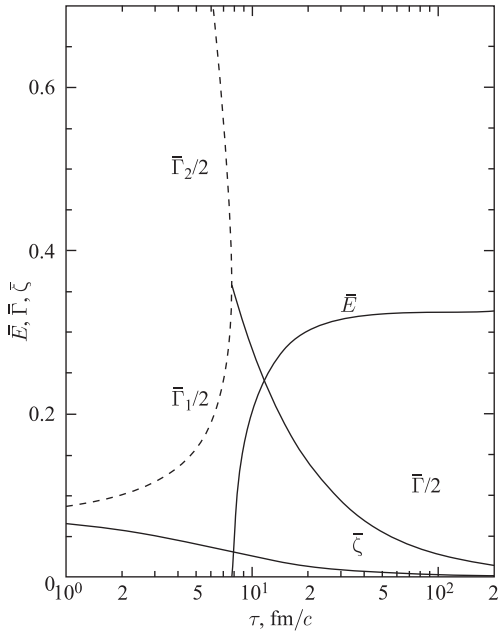

Fig. 9. Dependence upon relaxation time τ of the characteristic energy E and width Γ of oscillations and the instability growth rate parameter ζ for the case of Eq. (38) and for damping parameters Γ_1 and Γ_2 in the case of the solution given by Eq. (39). The dimensionless values of E, Γ, and ζ are shown in units of Fermi energy ϵ_F, i.e., $\overline{E} = E/\epsilon_F$, $\overline{\Gamma} = \Gamma/\epsilon_F$, and $\overline{\zeta} = \zeta/\epsilon_F$

We point out that the behavior of the friction coefficient γ in the above-mentioned relaxation regimes is essentially different. In the rare collision regime $\omega_F\tau \gg 1$, the friction coefficient γ in the equation of motion (36) is obtained from Eq. (35) as $\gamma = B^*/\tau \sim 1/\tau$. This τ dependence of the friction coefficient, $\gamma \sim 1/\tau$, is caused by the dynamic Fermi-surface distortions and it is opposite to the τ dependence of $\gamma \sim \tau$ in the short relaxation regime $\omega_F\tau \ll 1$ (see above).

We also point out that the presence of the characteristic oscillations of the bubble radius behind the barrier with $R > R^*$ can lead to the emission of γ quanta because of charged nuclear Fermi liquid. The energy, $E = \hbar\omega_R$, and the damping, $\Gamma = 2\hbar\omega_I$, of this radiation depend on both the phase transition, T_0, and the overheating, δT, temperatures. This fact can be used for the determination of both temperatures T_0 and δT from the measurement of the characteristics E and Γ of the corresponding resonance line. For the uncharged nuclear matter, the energy E and the damping parameter Γ are given in Fig. 1.

CONCLUSIONS

Starting from kinetic consideration, we have reduced the collisional kinetic equation for the Wigner distribution function $f(\mathbf{r}, \mathbf{p}; t)$ to the equations of motion for several local quantities: the particle density ρ, the velocity field, $\mathbf{u}$ and the pressure tensor $P_{\nu\mu}$. The structure of these equations significantly depends on the distortion of the Fermi surface in momentum space. The obtained equations of motion have, in general, a non-Markovian form. The memory kernel depends here on the relaxation time and provides a connection between both limiting cases of the classical liquid dynamics (short relaxation time limit) and the quantum Fermi-liquid dynamics (long relaxation time limit). The origin of the memory phenomenon in Fermi-liquid dynamics can be easily understood if we take into consideration the following fact. In the finite Fermi liquid, the deformation of the surface of the liquid drop or the distortion of the particle density in $\mathbf{r}$ space lead to the distortion of the Fermi surface in $\mathbf{p}$ space in each point of the liquid drop. On the distorted Fermi surface, the interparticle collisions are possible producing the two-body relaxation and the damping. That leads to the retarded damping of the basic motion in $\mathbf{r}$ space.

The Markovian dynamics exists in two above-mentioned limiting cases only. We also point out that the short-relaxation-time limit corresponds to the first sound propagation in an infinite Fermi liquid. In the opposite case of rare collision, one obtains a zero sound propagation with a strong renormalized sound velocity. Moreover, in the case of a finite drop dynamics, the deformation energy of the Fermi-liquid drop growth significantly when compared to the corresponding one in the classical liquid drop.

An important consequence of the Fermi-surface distortion is the fact that the interparticle collisions and the memory effects contribute to both the conservative and the dissipative parts of the equations of motion for the local quantities ρ, $\mathbf{u}$, and $P_{\nu\mu}$. The memory effects are especially important for a proper description of the transition from the zero-sound regime at low temperature to the first-sound regime at high temperatures. The memory effects influence strongly the nuclear collective motion increasing the nuclear stiffness coefficients and allowing us to describe the nuclear giant resonances (volume and surface collective modes).

It was shown in Sec. 4 that the memory effects influence significantly the development of instability near the fission barrier for a large enough relaxation time. The memory integral brings an additional elastic force which acts against the adiabatic driving force, leading to a hindrance of the drift of the nucleus from the barrier to the scission point and inducing characteristic shape oscillations of the nucleus. In general, the Fermi surface distortions and the memory effects lead to an important consequence of hindrance of the collective motion and, in particular, the nuclear fission. This hindrance occurs due to the time-reversible

elastic force caused by the memory integral and it represents an additional effect beside the hindrance due to the usual time-irreversible friction force.

We have studied the development of the bubble instability of heated nuclear matter and showed that the bubble instability and boiling of Fermi liquid itself are strongly influenced by the memory effects also, if the relaxation time is large enough. In this last case, an expansion of the bubble is accompanied by characteristic shape oscillations of the bubble radius which depend on the parameters of the memory kernel and the relaxation time. The oscillations of the bubble radius are due to the elastic force induced by the memory integral. This elastic force acts against the usual adiabatic force and hinders the growth of the bubble radius. In contrast to the case of the Markovian motion, the delay in the boiling process is caused here by both the conservative elastic and the friction forces.

REFERENCES

1. *Brown G. E.* Landau, Brueckner–Bethe, and Migdal Theories of Fermi Systems // Rev. Mod. Phys. 1971. V. 43. P. 1–14.
2. *Shlomo S., Kolomietz V. M.* Hot Nuclei // Rep. Progr. Phys. 2005. V. 68, No. 1. P. 1–76.
3. *Ring P., Schuck P.* The Nuclear Many-Body Problem. Berlin: Springer-Verlag, 1980.
4. *Kolomietz V. M.* Quantum Nuclear Hydrodynamics in the Mean-Field Approximation // Sov. J. Nucl. Phys. 1983. V. 37, No. 3. P. 325–331.
5. *Abrikosov A. A., Khalatnikov I. M.* The Theory of a Fermi Liquid // Rep. Progr. Phys. 1959. V. 22. P. 329–367.
6. *Soloviev V. G.* Theory of Complex Nuclei. M.: Nauka, 1971.
7. *Di Toro M.* Semiclassical Approach to the Description of Nuclear Collective Motion // Phys. Part. Nucl. 1991. V. 22, No. 2. P. 385–435.
8. *Balbutsev E. B., Mikhailov I. N.* Description of Collective Motion of Atomic Nuclei by the Moments Method // Collective Nuclear Dynamics (in Russian). Leningrad, 1989. P. 3–66.
9. *Balbutsev E. B.* Method of Moments and Nuclear Collective Motion // Phys. Part. Nucl. 1991. V. 22, No. 2. P. 333–384.
10. *Kolomietz V. M., Tang H. H. K.* Microscopic and Macroscopic Aspects of Nuclear Dynamics in Mean-Field Approximation // Phys. Scripta. 1981. V. 24, No. 6. P. 915–924.
11. *Nix J. R., Sierk A. J.* Microscopic Description of Isoscalar Giant Multipole Resonances // Phys. Rev. C. 1980. V. 21, No. 1. P. 396–404.
12. *Kiderlen D., Kolomietz V. M., Shlomo S.* Nuclear Shape Fluctuations in Fermi-Liquid Drop Model // Nucl. Phys. A. 1996. V. 608, No. 1. P. 32–48.

13. *Kolomietz V. M., Shlomo S.* Sound Modes in Hot Nuclear Matter // Phys. Rev. C. 2001. V. 64, No. 4. P. 044304(9).

14. *Lifshits E. M., Pitaevsky L. P.* Physical Kinetics. Oxford: Pergamon Press, 1993.

15. *Hasse R. W., Myers W. D.* Geometrical Relationships of Macroscopic Nuclear Physics. Berlin: Springer-Verlag, 1988.

16. *Bohr A., Mottelson B. R.* Nuclear Structure. V. 2. N. Y.: Benjamin, 1975.

17. *Migdal A. B.* Quadrupole and Dipole γ Radiation of Nuclei // Zh. Eksp. Teor. Fiz. 1948. V. 15, No. 1. P. 81.

18. *Vautherin D., Brink D. M.* Hartree–Fock Calculations with Skyrme's Interaction // Phys. Rev. C. 1972. V. 5, No. 3. P. 626–647.

19. *Kolomietz V. M., Shlomo S.* Low Density Instability in a Nuclear Fermi-Liquid Drop // Phys. Rev. C. 1999. V. 60, No. 4. P. 044612(6).

20. *Brack M. et al.* «Funny Hills». The Shell-Correction Approach to Nuclear Shell Effects and Its Applications to the Fission Process // Rev. Mod. Phys. 1972. V. 44, No. 2. P. 320–405.

21. *Ivanyuk F. A., Kolomietz V. M., Magner A. G.* Liquid-Drop Surface Dynamics for Large Nuclear Deformations // Phys. Rev. C. 1995. V. 52, No. 2. P. 678–684.

22. *Kolomietz V. M., Radionov S. V., Shlomo S.* Memory Effects on Descent from Nuclear Fission Barrier // Phys. Rev. C. 2001. V. 64, No. 5. P. 054302(11).

23. *Frenkel J.* Kinetic Theory of Liquids. Oxford: Clarendon Press, 1946.

24. *Landau L. D., Lifshitz E. M.* Statistical Physics. Oxford: Pergamon Press, 1958.

25. *Lamb H.* Hydrodynamics, Art 91a. N. Y.: Dover Publ., 1932.

26. *Kolomietz V. M., Sanzhur A. I., Shlomo S.* Non-Markovian Effects on the Dynamics of Bubble Growth in Hot Asymmetric Nuclear Matter // Phys. Rev. C. 2003. V. 68, No. 2. P. 014614(11).